Available online at www.sciencedirect.com
ScienceDirect
Ceramics International 35 (2009) 1083–1093
CERAMICS INTERNATIONAL
www.elsevier.com/locate/ceramint

In vitro bioactivity of glass–ceramics of the $CaMgSi_2O_6$–$CaSiO_3$–$Ca_5(PO_4)_3F$–Na_2SiO_3 system with TiO_2 or ZnO additives

S.M. Salman *, S.N. Salama, H. Darwish, H.A. Abo-Mosallam

Glass Research Department, National Research Centre, El-Behoos St., Dokki, Cairo 12622, Egypt

Received 10 September 2007; received in revised form 11 February 2008; accepted 29 April 2008
Available online 15 July 2008

Abstract

Glass–ceramic materials based on diopside [$CaMgSi_2O_6$]–wollastonite [$CaSiO_3$]–fluoroapatite [$Ca_5(PO_4)_3F$]–sodium silicate [Na_2SiO_3] system with TiO_2 or ZnO additives were successfully prepared and examined *in vitro*, by using a simulated body fluid (SBF) solution, to be suitable for restorative dental and bone implant materials. *In vitro* bioactivity of the glass–ceramics was examined by using scanning electron microscopy equipped with energy dispersive X-ray detectors (EDAX–SEM) and inductive coupled plasma emission spectroscopy (ICP).

The addition of TiO_2 showed a great positive effect on the bioactivity behaviour of the crystallized sample, while introducing ZnO to the glass led to decrease the rate of apatite formation on the corresponding glass–ceramic sample. *In vitro* test of glass–ceramics containing sodium calcium silicate solid solution showed higher bioactivity than that containing fluoroapatite. This fact indicated that the sodium calcium silicate solid solution has higher bioactive index than fluoroapatite.

The coefficients of thermal expansion of the obtained glass–ceramic materials are between 97×10^{-7} K^{-1} and 127×10^{-7} K^{-1} in the 25–600 °C temperature range and the Vicker's microhardness values are between 4635 MPa and 6615 MPa.

Keywords: Glass–ceramics; Bioactivity; SBF; Thermal expansion; Microhardness

1. Introduction

Since the first discovery of bioglass by Hench et al. [1], glass–ceramics have attracted more and more attentions in biomedical application. Natural bone and teeth are multiphase materials; their combination of properties probably can be simulated only by multiphase materials. Crystallization of glasses seems to be a very effective way to simulate hard tissues for those applications where elastic modulus mismatch and toughness are not important [2].

Apatite-based material has attracted considerable interest for orthopedic [3] and dental applications [4] because of their biocompatibility and tight bonding to bone, resulting in the growth of healthy tissue directly onto their surface. Several combinations between apatite and other phases have been proposed in order to improve the poor mechanical properties of apatite [5]. Hench [6] developed bioactive glasses and glass–ceramics of composition 45 SiO_2, 24.5 CaO, 24.5 Na_2O and 6 P_2O_5 wt%. Hydroxyl-apatite and apatite were the main crystal phases of the glass–ceramics. Kokubo et al. [7] prepared an apatite–wollastonite (A–W) glass–ceramics comparable to natural bone. This glass exhibits better mechanical properties than other bioceramics and is able to strongly bond with bone.

The system $Ca_5(PO_4)_3F$–$CaMgSi_2O_6$ provides fundamental knowledge for the development of new kinds of ceramics, glasses and bioglass–ceramics [8]. It is claimed that the $Ca_5(PO_4)_3F$–$CaMgSi_2O_6$ glass–ceramics show a combination of high mechanical strength, a high chemical resistance, and good biocompatibility [9]. Salama et al. [10] prepared a new bioglass–ceramics based on the stoichiometric compositions of 75 $CaMgSi_2O_6$–25 $Ca_5(PO_4)_3F$, with minor amounts of Na_2O, B_2O_3 and TiO_2. Salinas et al. [2] manufactured a bioactive glass–ceramics from $3CaO{\cdot}P_2O_5$–$CaO{\cdot}SiO_2$–$CaMgSi_2O_6$ ternary system.

Bioactivity can be defined as spontaneous communication of materials in biological environment resulting in strong adhesion between tissue and the materials [11]. However, it should be stressed that bioactivity is not only a specific material

* Corresponding author. Fax: +20 2 3370931.
E-mail address: hussein25@yahoo.com (S.M. Salman).

0272-8842/$34.00
doi:10.1016/j.ceramint.2008.04.025

property but also depends on the solution used for *in vitro* tests. Many efforts have been made by researchers to investigate the effect of solution type and materials composition on hydroxyl carbonate apatite (HCA) layer formation [12]. TiO_2 is one of the most common nucleating agents. The formation of bone-like apatite on artificial materials is induced by functional groups such as Si–OH and Ti–OH [13]. Salama et al. [10] found that the addition of TiO_2 enhanced the bioactivity behaviour of glass–ceramics.

The introduction of small amounts of zinc oxide in bioactive glass–ceramic materials for artificial bone could promote the wounds to heal and increase the immunity of the human bodies. Zinc oxide is an essential trace element that has stimulatory effects on bone formation [14]. Kamitakahara et al. [15] reported that the addition of zinc oxide to the bioactive glass–ceramics controls the reaction between the bioactive glass–ceramics and the surrounding body fluid.

The aim of the present work is to prepare varieties of bioglass–ceramic materials characterized by suitable chemical, biological, thermal and mechanical properties based on various contents of the stoichiometric compositions of diopside ($CaMgSi_2O_6$), fluoroapatite [$Ca_5(PO_4)_3F$], wollastonite ($CaSiO_3$), and sodium silicate (Na_2SiO_3) systems modified by the addition of TiO_2 or ZnO.

2. Experimental

2.1. Glass composition and preparation

The glass compositions were calculated to give different proportions of diopside [$CaMgSi_2O_6$]–wollastonite [$CaSiO_3$]–fluoroapatite [$Ca_5(PO_4)_3F$]–sodium silicate [Na_2SiO_3]. The calculated weight percentages of sodium silicate were gradually increased from 5% to 25% at the expense of wollastonite and at constant contents of fluoroapatite and diopside phases. The base glass composition (i.e. G_1) was modified by the addition of TiO_2 or ZnO over 100 g glass oxides, i.e. G_2 and G_3. The chemical compositions of the prepared glasses are given in Table 1.

Appropriate weight of reagent grade powders of $CaCO_3$, SiO_2 (quartz), $MgCO_3$, $NH_4{\cdot}H_2PO_4$, CaF_2, Na_2CO_3, ZnO, and TiO_2 were thoroughly mixed and melted in Pt–2%Rh crucible in an electric furnace with SiC heating elements at 1350–1450 °C for 4 h. Melting was continued until clear homogeneous melt was obtained; this was achieved by swirling the melt several times at about 30-min interval. The melt was cast into rods and as buttons, which were then properly annealed in a muffle furnace at 500 °C to minimize the strain.

2.2. Differential thermal analysis (DTA)

The thermal behaviour of the finely powdered glass sample was examined using the SETARAM Labsys^{TM} TG-DSC16. The powdered sample was heated in Pt holder with another Pt holder containing α-Al_2O_3 as a standard material. A uniform heating rate of 10 °C min^{-1} was adopted up to the appropriate temperature of the glasses. The results obtained were used as a guide to determine the temperatures for the heat treatment applied to induce crystallization of the glasses.

2.3. Thermal treatment

The progress of crystallization in the glasses was followed using double stage heat-treatment regimes. Crystallization was carried out at temperatures in the region of the main DTA exothermic peak determined for each glass. The glasses were first heated according to the DTA results at the endothermic peak temperature for 5 h, and then were followed by another thermal treatment at the exothermic peak temperature for 10 h.

2.4. Material investigation

Identification of crystal phases precipitating during the course of crystallization was done by examining X-ray diffraction patterns obtained by using XSPEX, X-ray diffractometer with search/match option, version 5.45, Diano Corporation, Woburn, MA, USA. The crystallization characteristics and internal microstructure of the resultant materials were examined by using scanning electron microscopy (SEM), where electron micrographs of representative samples were obtained using Jeol, JXA-840 on electron probe microanalyzer scanning electron microscope.

2.5. Properties

2.5.1. Thermal expansion measurements

The coefficients of thermal expansion of the investigated glass–ceramic samples were carried out on 1.5–2.0-cm long

Table 1
Theoretical phase constituents and the respective oxide components of the glasses

Glass no.	Theoretical phase constituents (wt%)				Oxide constitutions (mol%)						Additives in g over 100 g glass oxide	
	Dio	FA	Wo	NaS	CaO	MgO	Na_2O	SiO_2	P_2O_5	CaF_2	ZnO	TiO_2
G_1	50	25	20	5	37.45	13.81	2.45	40.36	4.44	1.49	–	–
G_1–T	50	25	20	5	37.45	13.81	2.45	40.36	4.44	1.49	–	3.0
G_1–Z	50	25	20	5	37.45	13.81	2.45	40.36	4.44	1.49	3.0	–
G_2	50	25	10	15	32.46	13.88	7.39	40.31	4.47	1.49	–	–
G_3	50	25	–	25	27.42	13.95	12.37	40.27	4.49	1.50	–	–

Dio = diopside, FA = fluoroapatite, Wo = wollastonite, NaS = sodium silicate.

Table 2
Ionic concentrations (mM) in the simulated body fluid (SBF) solution and human plasma

Occurrence	Ions concentrations (mM)							
	Na^+	K^+	Mg^{2+}	Ca^{2+}	Cl^-	HCO^-	HPO_4^{2-}	SO^{4-}
Human plasma	142.0	5.0	1.5	2.5	103.0	27.0	1.0	0.5
SBF solution	142.0	5.0	1.5	2.5	147.8	4.2	1.0	0.5

rods using Linseis L76/1250 automatic recording multiplier dilatometer with a heating rate of 5 °C min^{-1}. The linear thermal expansion coefficient was automatically calculated using the general equation:

$$\alpha = \left(\frac{\Delta L}{L}\right)\left(\frac{1}{\Delta T}\right)$$

where ΔL is the increase in length, ΔT is the temperature interval over which the sample is heated and L is the original length of the specimen.

2.5.2. Microhardness measurements

The microhardness of the investigated samples was measured by using Vicker's microhardness indenter (Model

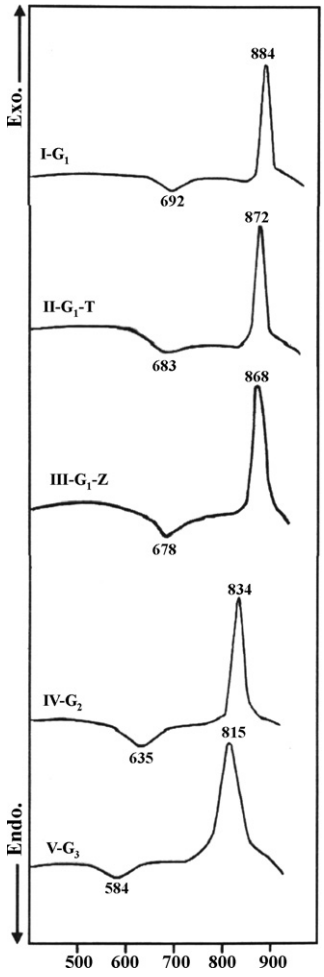

Fig. 1. DTA data of the glasses.

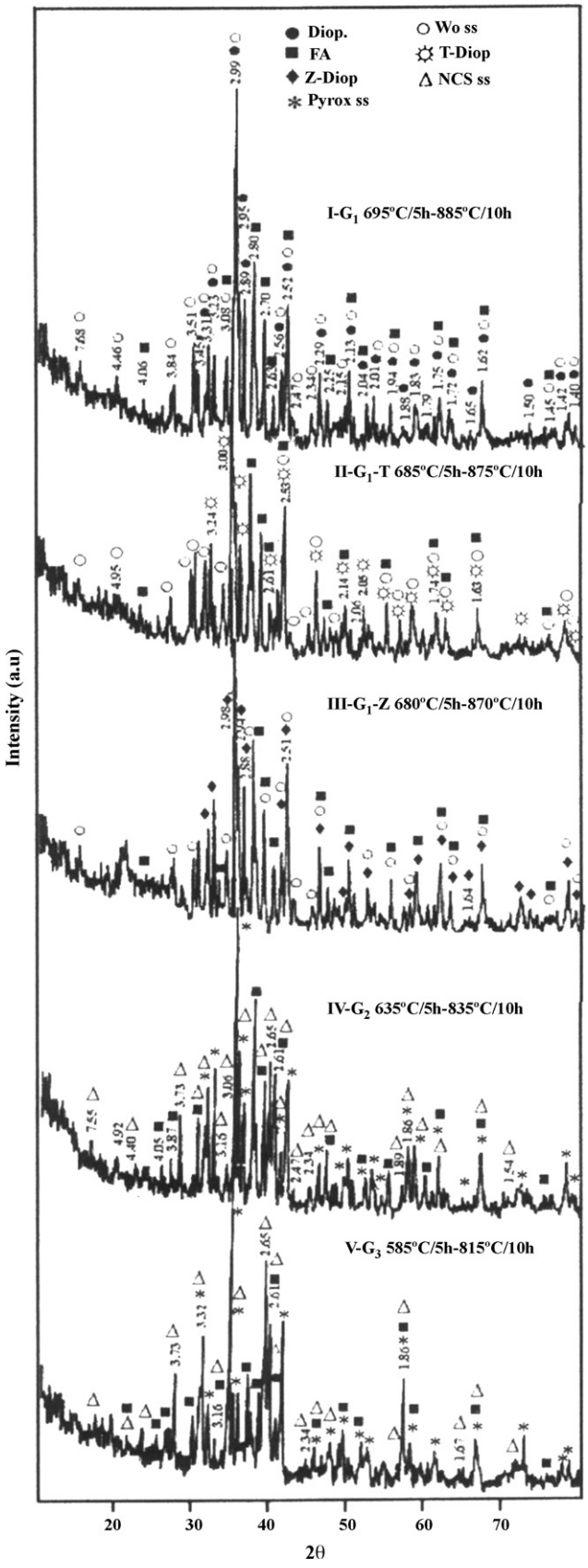

Fig. 2. XRD analysis of crystallized glasses.

HV-100 microhardness tester). The eyepiece on the microscope of the apparatus allowed measurements with an estimated accuracy of ±0.5 μm for the indentation diagonals. The specimens were cut using a low speed diamond saw, dry ground and polished carefully to obtain smooth and flat parallel surfaces of glass–ceramic samples before indentation testing. At least six indentation readings were made and measured for each sample. Testing was made using a load of 100 g; loading time was fixed for all glasses and crystalline samples (15 s). The measurements were carried out under normal atmospheric conditions. The Vicker's microhardness value was calculated from the following equation:

$$H_v\,(\mathrm{kg/mm^2}) = A\left(\frac{P}{d^2}\right)$$

where A is a constant equal to 1854.5 takes into account the geometry of squared-based diamond indenter with an angle 136° between the opposing faces, P is the applied load (g) and d is the average diagonal length (μm). The microhardness values are converted from kg/mm^2 to MPa by multiplying with a constant value 9.8.

2.5.3. *In vitro* test

In *in vitro* bioactivity tests all the specimens were carried out in polyethylene containers soaking the samples at 37 ± 0.5 °C, for 7, 14, and 21 days in 50 ml of Tris-buffered simulated body fluid (SBF) solution, whose composition is shown in Table 2. Pieces were mounted vertically in a special polyethylene scaffold to avoid deposition by gravity. The SBF solution was prepared by dissolving reagent grade NaCl, $NaHCO_3$, KCl, $K_2HPO_4{\cdot}3H_2O$, $MgCl_2{\cdot}6H_2O$, $CaCl_2$, and Na_2SO_4 into deionized water. The solution was buffered to pH 7.4 with Tris-(hydroxymethyl)-aminomethane [$(CH_2OH)_3$ CNH_3] and hydrochloric acid. Surface modifications of the materials were studied by scanning electron microscope with energy dispersive X-ray analysis (SEM–EDAX) Model Philips XL 30. The variation of ion concentrations in the SBF solution after soaking the sample was monitored by using inductive coupled plasma (ICP) Model (Jobian Yvon Horiba Ultima 2000).

3. Results

The DTA data (Fig. 1) of the glass samples showed endothermic effects at the 584–692 °C temperature range. This effect represents the glass transition temperature (T_g), at which the atoms begin to arrange themselves in preliminary structure elements subsequent to crystallization. Exothermic effects observed at the 815–884 °C temperature range indicated that the crystallization reaction takes place in the glasses.

Investigation of the glass–ceramic materials by X-ray diffraction analysis revealed that predominant diopside ($CaMgSi_2O_6$), fluoroapatite $Ca_5(PO_4)_3F$, and wollastonite solid solutions were crystallized from the base glass (G_1, Fig. 2 Pattern I, Table 1). The addition of TiO_2 in the base glass, i.e. G_1–T, led to the crystallization of titanium diopside phase

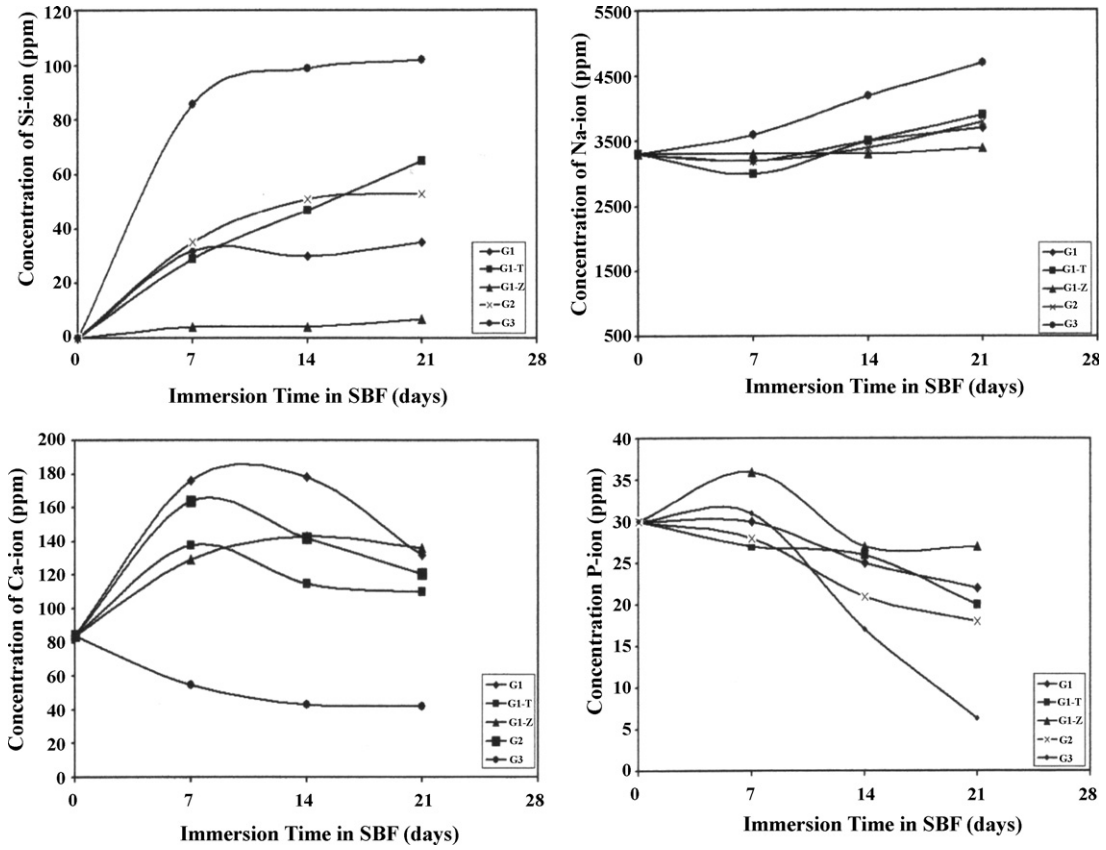

Fig. 3. changes in element concentrations of SBF solution due to soaking of glass–ceramic samples.

(Fig. 2, Pattern II). On the other hand, ZnO-containing base glass, i.e. (Fig. 2, Pattern III) crystallized predominantly into pyroxene solid solution (zincain diopside) together with fluoroapatite and wollastonite solid solutions.

The addition of 10 wt% and 20 wt% of sodium silicate (Na_2SiO_3) at the expense of wollastonite ($CaSiO_3$), i.e. G_2 and G_3, respectively led to the development of clinopyroxene solid solution ($MgSiO_3$–$CaMgSi_2O_6$), sodium calcium silicate solid solution and fluoroapatite phases (Fig. 2, Patterns IV and V).

Fig. 3 correlates the elemental concentrations of Ca, Na, Si, and P in SBF solution with the immersion time. All ion concentrations increased in the early stages of soaking in SBF solution (after 7 days). The amounts of silicon and sodium were increased, while calcium and phosphorous concentrations were decreased with immersion time. The depletion in calcium and phosphorous ions indicates that they are precipitating on the material surfaces.

Figs. 4–13 show SEM and EDAX spectra obtained from the glass–ceramic samples before and after soaking in SBF solution. SEM micrographs of the polished surfaces of the glass–ceramic specimens before soaking in the SBF solution are shown in Figs. 4a, 6a, 8a, 10a and 12a. These surfaces generally exhibited regular textures without pores.

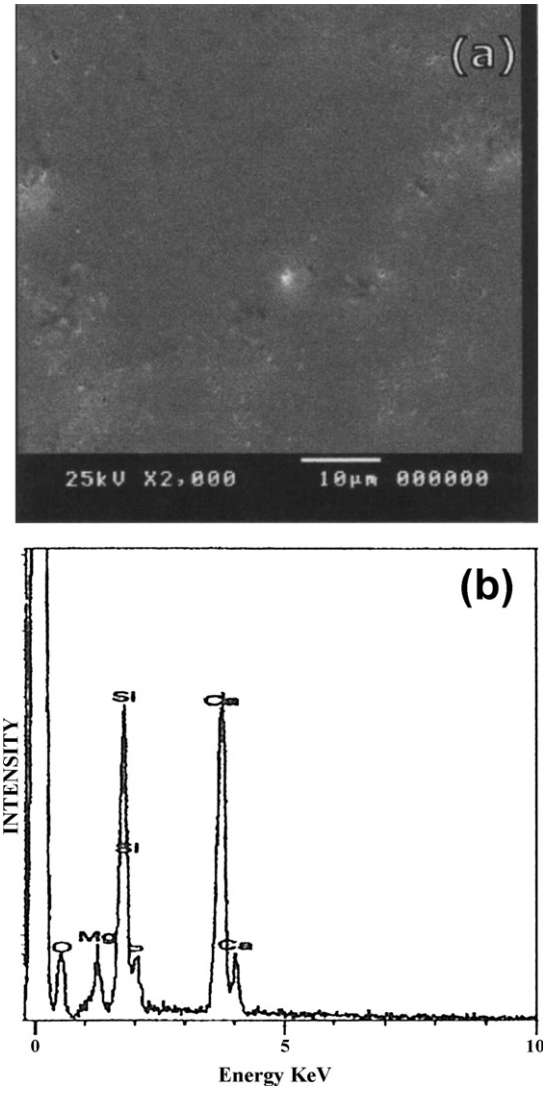

Fig. 4. (a) SEM micrograph and (b) EDAX of the glass–ceramic surface of specimen G_1 before the immersion in the SBF solution.

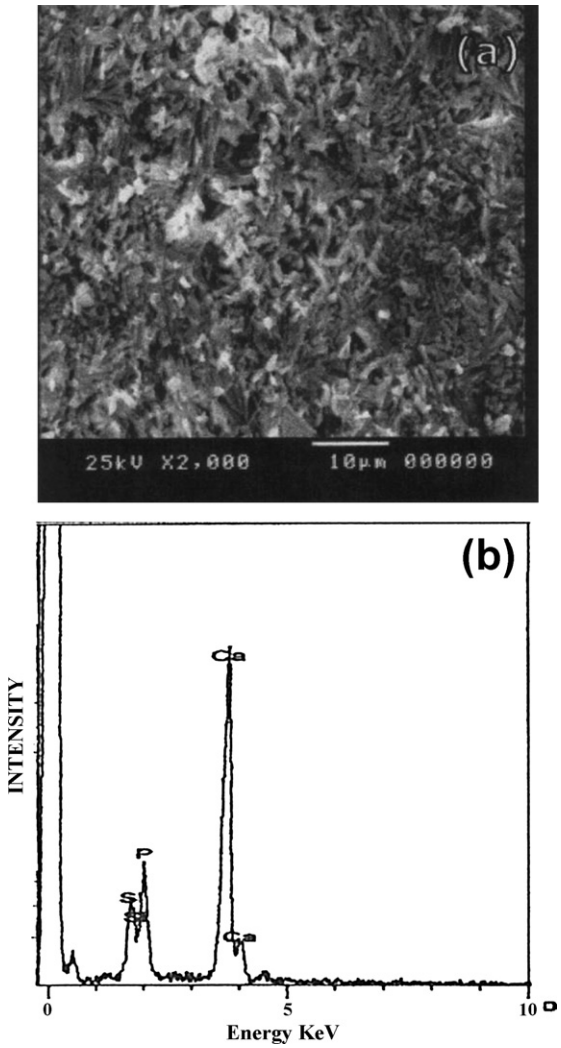

Fig. 5. (a) SEM micrograph and (b) EDAX of the glass–ceramic surface of specimen G_1 after the immersion in the SBF solution.

Apatite layer with different shapes and quantities were formed on all samples after immersion in the SBF solution for 21 days. Needle-like growths were observed on the surface of G_1 (Fig. 5a), while ball-like growths were presented on the surfaces of G_1–T and G_1–Z (Figs. 7a and 9a, respectively). Large cotton-like growths were formed in the surfaces of G_2 (with 10 wt% $CaSiO_3$), however the scanning electron micrograph (Fig. 13a) of G_3 (free of $CaSiO_3$) showed that the apatite layer is formed as ball-like texture.

Figs. 4b–13b show a comparison of the EDAX spectra of glass–ceramic surfaces before and after soaking in SBF solution. EDAX traces (Fig. 4b) collected from the surface of the sample G_1 before treatment in the SBF solution, showed the presence of Ca, Na, Mg, Si, and P elements. After immersion in the SBF solution for 21 days the EDAX spectra revealed that, layer rich in Ca and P but poor in Si was detected (Fig. 5b).

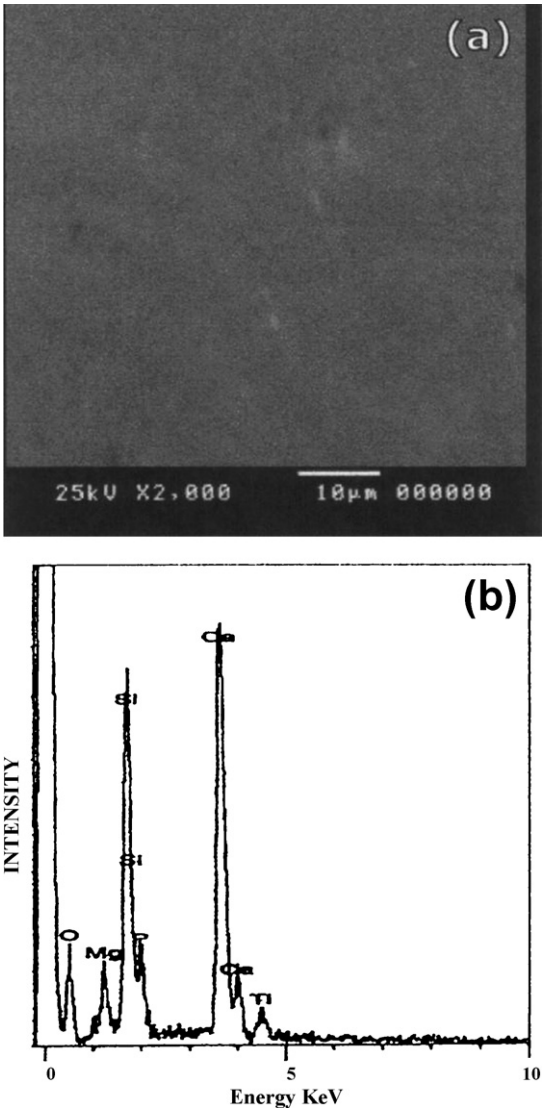

Fig. 6. (a) SEM micrograph and (b) EDAX of the glass–ceramic surface of specimen G_1–T before the immersion in the SBF solution.

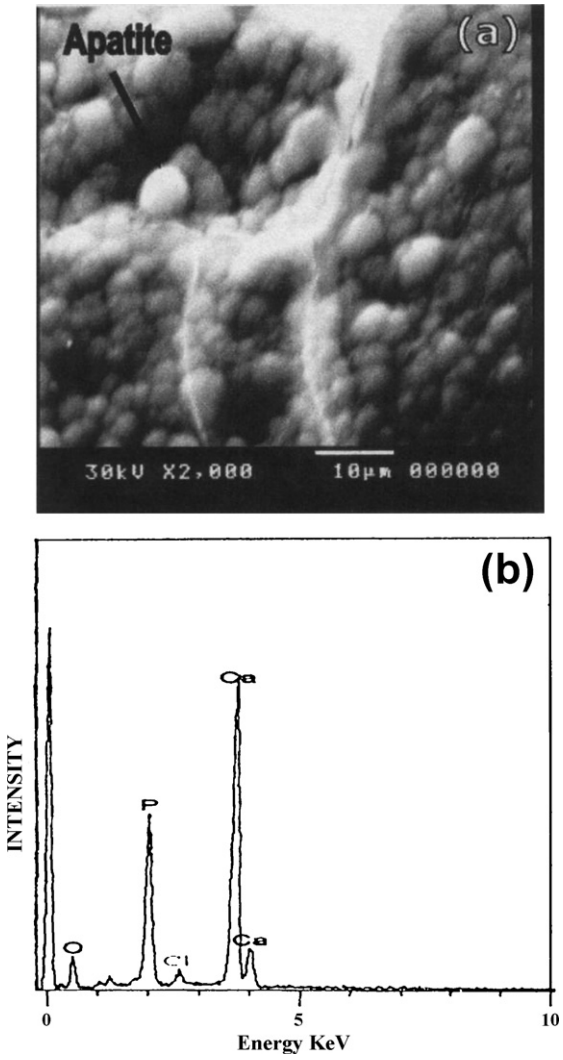

Fig. 7. (a) SEM micrograph and (b) EDAX of the glass–ceramic surface of specimen G_1–T after the immersion in the SBF solution.

A comparison of the EDAX spectra of G_1–T before and after soaking in SBF solution is illustrated in Figs. 6b and 7b, respectively. It was observed that the newly formed layer was mainly composed of calcium and phosphorous after soaking in SBF solution for 21 days. Fig. 8b the EDAX trace of the surface of glass–ceramic sample G_1–Z before soaking in the SBF solution, showed the presence of Ca, Na, Mg, Si, P, and Zn elements. After immersion in SBF solution (Fig. 9b) the EDAX spectra revealed that similar traces were obtained except the peak intensity of the phosphorous element that was longer than that of silicon peak.

The addition of Na_2SiO_3 instead of $CaSiO_3$ enhanced the development of apatite layer on the surfaces of the crystalline samples, i.e. (G_2 and G_3). Figs. 10b and 12b represented the EDAX spectra of the surfaces of glass–ceramic samples G_2 and G_3, respectively (before immersion in SBF solution). The presence of Ca, Na, Mg, Si, and P elements on the surface of the studied glass–ceramics was recorded. The change in the intensities of the EDAX spectra (Figs. 11b and 13b) obtained from the same samples after soaking in SBF solution showed that significant peaks of calcium and phosphorous were detected in the crystalline sample G_2. However, short peak of silicon was detected (Fig. 11b). Fig. 13b revealed that the intensity of phosphorous peak was increased, while the peak of silicon could not be detected.

The investigated glass–ceramics had microhardness values between 4635 MPa and 6615 MPa and thermal expansion coefficient values between $97 \times 10^{-7}\,K^{-1}$ and $127 \times 10^{-7}\,K^{-1}$ in the 25–600 °C temperature range.

A summary of the crystalline phases formed, the thermal and microhardness properties of the crystalline samples was illustrated in Table 3.

4. Discussion

It is apparent that, the ease of crystallization of the prepared glasses can be correlated to the presence of phosphate and silicate networks, and to the possible phase separation which took place in the glass even in microscale of the two phases

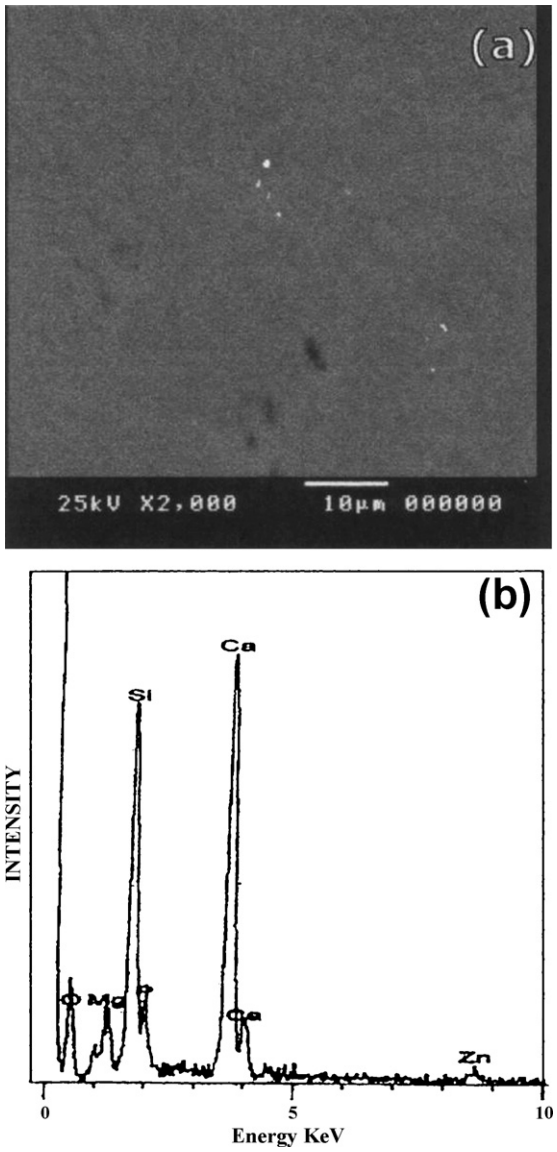

Fig. 8. (a) SEM micrograph and (b) EDAX of the glass–ceramic surface of specimen G_1–Z before the immersion in the SBF solution.

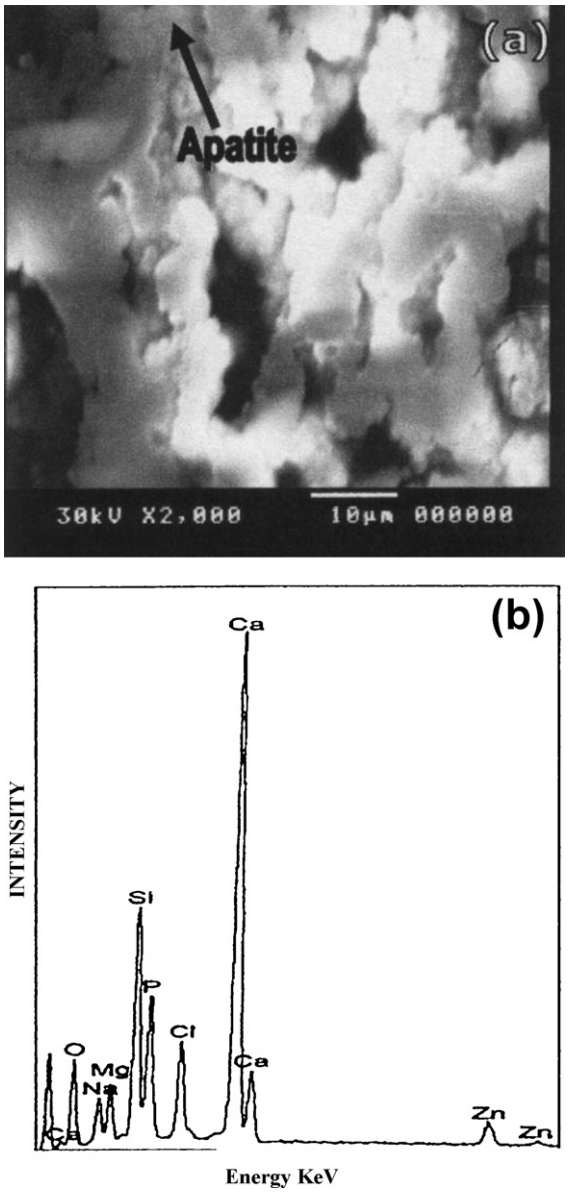

Fig. 9. (a) SEM micrograph and (b) EDAX of the glass–ceramic surface of specimen G_1–Z after the immersion in the SBF solution.

upon thermal treatment. It is well known that the addition of P_2O_5 to silicate glass composition promotes volume nucleation and glass–ceramic formation as indicated by McMillan [16].

The occurrence of the various phases formed in the present glasses was a function of the original glass compositions and the crystallization parameters used. Investigation of the glass–ceramic materials by X-ray diffraction analysis revealed that predominant diopside, fluoroapatite, and wollastonite solid solution phases were crystallized from the base G_1. The displacement of *d*-spacing lines of wollastonite-like phase towards higher 2θ value, gives an evidence that some of diopside phases are accommodated in wollastonite forming wollastonite solid solution [17].

Mineralogically, the addition of TiO_2 or ZnO in the base glass, i.e. G_1–T or G_1–Z, respectively led to enhance the crystallization of pyroxene solid solution (diopsidic-type) instead of the proper diopside. This may be attributed to the tendency of diopside to accumulate titanium [18] or zinc [19] in its structure to form the solid solution.

On increasing of Na_2SiO_3 at the expense of $CaSiO_3$ in the glasses G_2 and G_3, sodium calcium silicate solid solution phase was developed together with pyroxene solid solution and fluoroapatite phases. The present results, indicated that sodium calcium silicate solid solution was developed instead of fluoroapatite ($Ca_5(PO_4)_3F$) phase, as indicated from the shift of *d*-spacing lines of XRD characteristics of the $Na_2Ca_2Si_3O_9$ phase towards higher 2θ values and the decrease of the intensity of fluoroapatite phase. It seemed, therefore, that there is a preferential tendency of sodium calcium silicate ($Na_2Ca_2Si_3O_9$) to capture P_2O_5 in its structure [20].

Among implantable materials, some are known to form a strong chemical bond with bone. Bone bonding is restricted to surface reactive materials, the so-called bioactive materials.

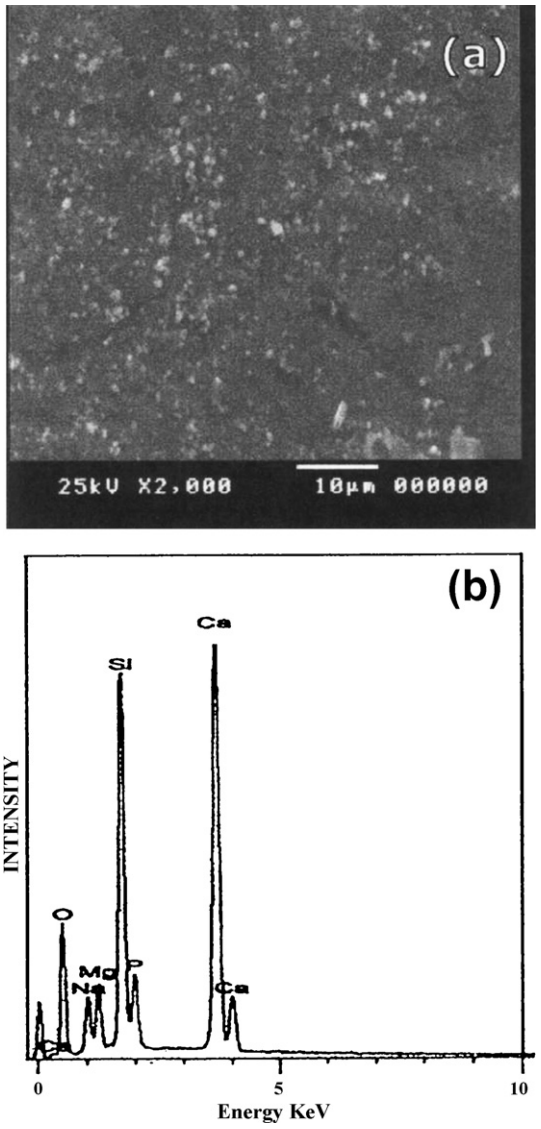

Fig. 10. (a) SEM micrograph and (b) EDAX of the glass–ceramic surface of specimen G_2 before the immersion in the SBF solution.

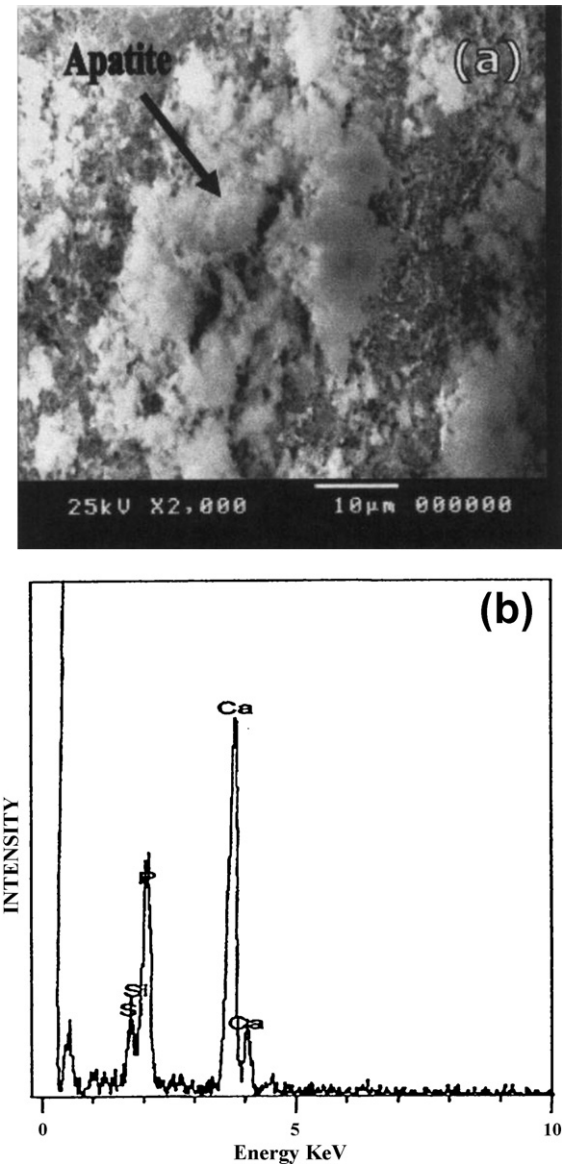

Fig. 11. (a) SEM micrograph and (b) EDAX of the glass–ceramic surface of specimen G_2 after the immersion in the SBF solution.

Bioactivity is thought to be a result of the chemical composition of the biomaterials, based on leaching, dissolution, and precipitation [21]. The *in vitro* study in the SBF solution of the glass–ceramic samples revealed that each one showed different bioactivity behaviours in *in vitro* test.

The mechanism of apatite formation on $CaO–SiO_2$-based glasses in SBF solution had been previously reported by Ohtsuki et al. [22]. Briefly, when implant materials are exposed to SBF solution, calcium ions are released from them and silanol groups are formed on their surfaces. The formed silanol groups seemed to induce heterogeneous nucleation of apatite. Moreover, the released calcium ions increase the degree of supersaturation by increasing the ionic activity product of apatite and accelerate apatite nucleation. Once apatite nuclei are formed, they grow spontaneously, since body fluid and SBF solutions are supersaturated with respect to apatite even under normal condition.

Fig. 3 shows the variation of elemental concentrations of Ca, Na, Si, and P in the SBF solution during the immersion of glass–ceramic samples. In the early stage of immersion, the glass–ceramic samples and the concentration of all ions were increased in the SBF solution. Therefore, the results obtained, suggested that interaction occurred relatively between the SBF solution and the glass–ceramic samples [10]. However, the release of silicon from the glass–ceramics significantly decreased with ZnO addition. This indicates that the reaction between the glass–ceramic sample (G_1–Z) and fluid was suppressed and formation of silanol groups was also suppressed. This may be attributed to the chemical durability of the glass–ceramic sample is improved by the addition of ZnO because of the nature of ZnO. ZnO is an amphoteric oxide and shows very low solubility in the SBF solution [15]. Therefore, the suppression of formation of silanol groups leads to the

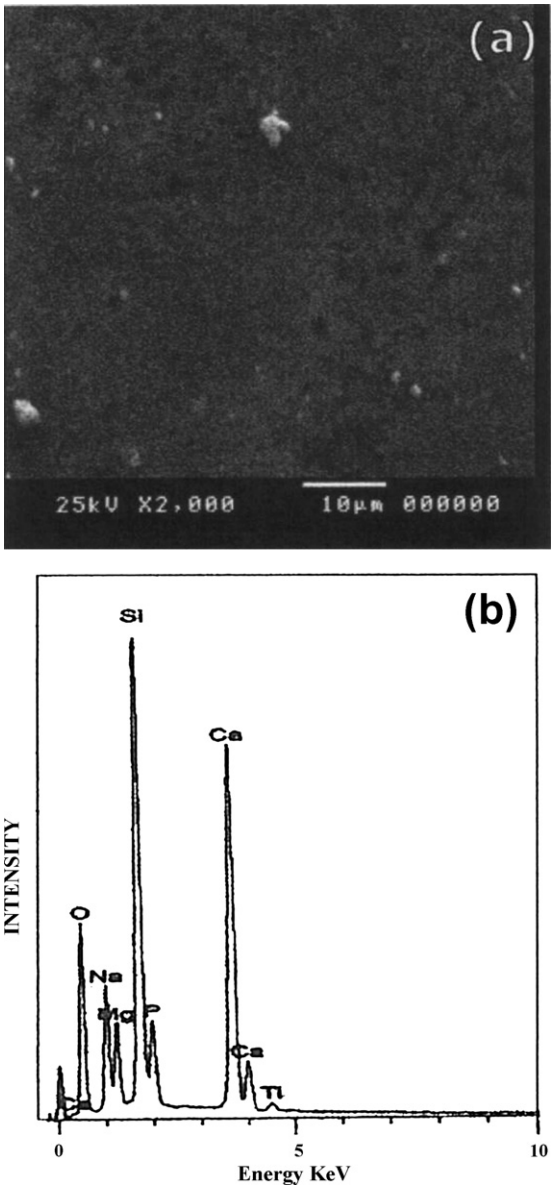

Fig. 12. (a) SEM micrograph and (b) EDAX of the glass–ceramic surface of specimen G_3 before the immersion in the SBF solution.

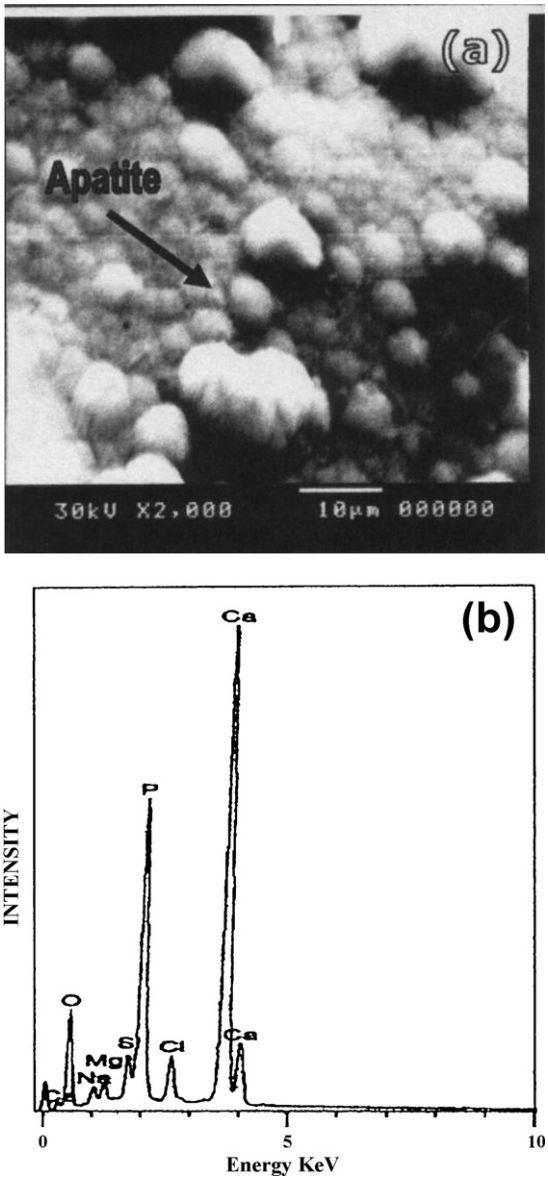

Fig. 13. (a) SEM micrograph and (b) EDAX of the glass–ceramic surface of specimen G_3 after the immersion in the SBF solution.

suppression of apatite formation on the glass–ceramics, as seen in the sample G_1–Z.

Depletion of Ca and P concentrations and the increase of the silicon in the SBF solution with the immersion time were observed, these changes of ion concentrations may be associated with the Ca–P rich layer formation. The decrease of calcium and phosphorous concentrations in the SBF solution during immersion of biomaterials indicates that they are precipitated on the material surface [23].

Table 3
Crystalline phases developed, thermal expansion and microhardness data of the investigated glass–ceramic materials

Sample no.	Microhardness (MPa)	Thermal expansion coefficients, α ($\times 10^{-7}$ K^{-1})					Heat-treatment (°C/h)	Phases developed
		25–200	25–300	25–400	25–500	25–600		
G_1	6262	94	96	99	102	106	695/5 h–885/10 h	Diop + FA + Wo ss
G_1–3T	6615	85	90	93	94	97	680/5 h–870/10 h	T-Diop + FA + Wo ss
G_1–3Z	6164	96	98	99	104	108	685/5 h–875/10 h	Z-Diop + FA + Wo ss
G_2	5586	99	103	107	109	111	635/5 h–835/10 h	Pyrox ss + FA + NCS ss
G_3	4635	106	116	121	123	127	585/5 h–815/10 h	Pyrox ss + NCS ss + FA

Diop = diopside, FA = fluoroapatite, Wo ss = wollastonite solid solution, T-Diop = titanium diopside, Z-Diop = zincian diopside, NCS ss = sodium calcium silicate solid solution, Pyrox ss = pyroxene solid solution.

Further evidence to confirm the presence of apatite on the surfaces of glass–ceramic samples with different magnitude, was sought by using the EDAX and SEM techniques before and after the soaking in the SBF solution.

Fig. 4b is the EDAX trace from the surface of the base glass–ceramic G_1 before soaking in the SBF solution showing the presence of Ca, Mg, Si, and P. EDAX spectra from the same sample after immersion in the SBF solution for 21 days revealed that significant peaks for Ca and P and short peak for silica are due to the formation of the apatite layer [10].

The addition of TiO_2, i.e. G_1–T showed a great positive effect on the bioactivity behaviour of the crystallized sample. It is clear that the bioactivity of the studied glass–ceramic sample containing TiO_2, i.e. G_1–T was higher than that sample TiO_2-free (e.g. G_1) as indicated from the EDAX patterns (Figs. 5b and 7b respectively). Fig. 6b revealed that the peak for silica was disappeared, i.e. the surface of G_1–T sample was completely covered with apatite layer as compared with G_1 (Figs. 5a and 7a respectively). This can be explained on the basis that the formation of Ti–OH groups on the surface of biomaterials after soaking in SBF solution exhibits negative charge and hence, it combines selectively with the positively charged Ca^{2+} ion in the fluid to form calcium titanate. Then, the surface, therefore, gradually gains an overall positive charge. As a result, the positively charged surface combines with the negatively charged phosphate ions from the SBF solution to form apatite layer [13].

On the other hand, the addition of ZnO to the base glass, i.e. G_1 decreases the bioactivity level of the corresponding glass–ceramic sample. It is clear that the bioactivity of the studied ZnO-containing glass–ceramic sample was lower than that of Zn-free sample as indicated from EDAX patterns and SEM micrographs. This may be due to the chemical durability of the glass–ceramic sample, which is improved by the addition of ZnO [15] and acts as a potent inhibitor of the crystal growth of apatite phase [24]. It should be mentioned that the addition of ZnO in small amount (i.e. 3 g) in the glass–ceramics has still showed apatite forming ability (Fig. 9a). The reaction between the glass–ceramics and body fluid governs not only its bioactivity, but also its biodegradability. This suggests that it can control the biodegradability of the glass–ceramics to some extent without losing its bioactivity.

The modification of the base glass by increasing sodium silicate Na_2SiO_3 component at the expense of wollastonite–$CaSiO_3$ component was found to increase the bioactivity level. This may be attributed to the formation of sodium calcium silicate solid solution phase (P_2O_5–$Na_2Ca_2Si_3O_9$) at the expense of fluoroapatite. Peitl et al. [20] demonstrated that *in vitro* tests that fully crystallized $Na_2Ca_2Si_3O_9$ glass–ceramics are much more bioactive than any commercial bioactive ceramics or other glass–ceramics. Hench et al. [25] found that the onset time for apatite layer formation for $Na_2Ca_2Si_3O_9$-containing glass–ceramics with 6 wt% P_2O_5 as solid solution was less than $Na_2Ca_2Si_3O_9$ without P_2O_5.

There was another evidence to confirm the increase of the bioactivity with Na_2SiO_3/$CaSiO_3$ replacement by using EDAX, SEM, and ICP techniques. It was found that the peak intensity of the EDAX pattern of the phosphorous was increased at the expense of silicon peak intensity by the addition of Na_2SiO_3 instead of $CaSiO_3$.

The SEM micrographs showed that the surfaces of the glass–ceramic samples G_2 and G_3 after the immersion for 21 days in the SBF solution were covered with the apatite layer (Figs. 11a and 13a). This was also supported by the ICP measurements, which showed that the concentrations of calcium and phosphorous elements in the SBF solution were decreased with the immersion time.

The thermal expansion coefficients (α-values) decreased and the microhardness increased of the glass–ceramic samples with the addition of TiO_2. While the addition of ZnO in sample G_1–Z and introduction of Na_2SiO_3 at the expense of $CaSiO_3$ in samples G_2 and G_3 increased the α-values and decreased the microhardness values of the studied crystalline samples. The α-values of the studied glass–ceramics are between $97 \times 10^{-7}\,K^{-1}$ and $127 \times 10^{-7}\,K^{-1}$ in the 25–600 °C temperature range and the microhardness values of these samples were between 4635 MPa and 6615 MPa. The glass–ceramics in the present study have high bioactivity, good thermal, and mechanical properties, i.e. they can be used in dental restoration and as bone implant materials.

5. Conclusions

Glass–ceramic materials based on diopside [$CaMgSi_2O_6$]–wollastonite [$CaSiO_3$]–fluoroapatite [$Ca_5(PO_4)_3F$]–sodium silicate [Na_2SiO_3] system with TiO_2 or ZnO additives were successfully prepared and examined *in vitro* to be suitable for restorative dental and bone implant materials.

The addition of TiO_2 showed a great positive effect on the bioactivity behaviour of the crystallized sample, while introduction of ZnO to the glass decreased the rate of apatite formation on the corresponding glass–ceramic sample. *In vitro* test glass–ceramics containing sodium calcium silicate solid solution phase showed higher bioactivity than that containing fluoroapatite phase. This fact indicated that sodium calcium silicate solid solution phase has high bioactive index than fluoroapatite phase.

References

[1] L.L. Hench, R.J. Splinter, W.C. Allen, T.K. Greenlee, Bonding mechanism at the interface of ceramic prosthetic materials, J. Biomed. Mater. Res. Symp. 2 (1971) 117–141.
[2] A.J. Salinas, J. Roman, M. Vallet-Regi, J.M. Oliveira, R.N. Correia, M.H. Fernandes, *In vitro* bioactivity of glass and glass ceramics of the $3CaO{\cdot}P_2O_5$–$CaO{\cdot}SiO_2$–$CaO{\cdot}MgO{\cdot}2SiO_2$ system, Biomaterials 21 (2000) 251–257.
[3] R.Z. LeGeros, J.P. LeGeros, Dense hydroxyapatite, in: L.L. Hench, J. Wilson (Eds.), An Introduction to Bioceramics: Advanced Series in Ceramics, vol. 1, World Scientific, Singapore, 1993, pp. 139–180.
[4] Z. Strnad, Recent progress in bioactive ceramics for medical application in Czech Republic, in: Proceedings of the Fifth ESG Conference, Prague, (June 1999), pp. 2–8.
[5] S. Agathopoulos, D.U. Tulyaganov, P.A.A.P. Marques, M.C. Ferro, M.H.V. Fernandes, R.N. Correia, The fluoroapatite–anorthite system in biomedicine, Biomaterials 24 (2003) 1317–1331.
[6] L.L. Hench, Bioceramics: from concept to clinic, J. Am. Ceram. Soc. 74 (7) (1991) 1485–1510.

[7] T. Kokubo, M. Shigematsu, Y. Nagashisma, M. Tashiro, T. Nakamura, T. Yamamuro, S. Higashi, Apatite- and wollastonite-containing glass–ceramics for prosthetic application, Bull. Inst. Chem. Res., Kyoto Univ. 60 (3–4) (1982) 260–268.
[8] D.U. Tulyaganov, Phase separation and devitrification in the fluoroapatite–diopside system, in: Proceedings of the XIX International Congress on Glass, 1-6 July, vol. 2, Extended Abstract, Edinburgh, Scotland, 2001„ p. 198.
[9] D.U. Tulyaganov, M. Aripova, Bioactive glass–ceramic containing anorthite and diopside, in: Proceedings of the XVI International Congress on Glass, Bol. Soc. ESP Ceram. VID, 31-C, vol. 5, 1992, pp. 227–232.
[10] S.N. Salama, H. Darwish, H.A. Abo-Mosallam, HA forming ability of some glass–ceramics of the $CaMgSi_2O_6$–$Ca_5(PO_4)_3F$–$CaAl_2SiO_6$ system, Ceram. Int. 32 (2006) 357–364.
[11] L.L. Hench, Bioactive materials: the potential for tissue regeneration, J. Biomed. Mater. Res. 41 (4) (1998) 511–518.
[12] L.L. Hench, G. La-Torre, Reaction kinetics of bioactive ceramics, part IV: effect of glass and solution composition, in: T. Yamamuro, T. Kokubo, T. Nakamura (Eds.), Bioceramics, Kobonshi Kankokai, Inc., Kyoto, Japan, 1992, pp. 67–74.
[13] T. Kokubo, H.M. Kim, M. Kawashita, Novel bioactive materials with different mechanical properties, Biomaterials 24 (2003) 2161–2175.
[14] M. Yamaguchi, H. Oishi, Y. Suketa, Stimulatory effect of zinc on bone formation in tissue culture, Biochem. Pharmacol. 36 (1987) 4007–4012.
[15] M. Kamitakahara, C. Ohtsuki, H. Inada, M. Tanihara, T. Miyazaki, Effect of ZnO addition on bioactive CaO–SiO_2–P_2O_5–CaF_2 glass–ceramics containing apatite and wollastonite, Acta Biomater. 2 (2006) 464–471.
[16] P.W. McMillan, Glass–Ceramics, Academic Press, London, NY, 1979.
[17] W.A. Deer, R.A. Howie, Zussman, An Introduction to the Rock Forming Minerals. Third ELBS Impression, Common Wealth, Printing Press Ltd., Hong Kong, 1992.
[18] S.N. Salama, Glass ceramics containing some varieties of Mn-solid solution phases, Mater. Chem. Phys. 28 (1991) 237.
[19] E.J. Essene, D.R. Peacor, Petedunnite ($CaZnSi_2O_6$), a new zinc clinopyroxene from Franklin, New Jersey, and phase equilibria for zincian pyroxenes, Am. Miner. 72 (1987) 157–166.
[20] O. Peitl, E.D. Zanotto, L.L. Hench, Highly bioactive P_2O_5–Na_2O–CaO–SiO_2 glass–ceramics, J. Non-Cryst. Solids 292 (2001) 115–126.
[21] C. Loty, J.M. Sautier, H. Boulekbache, T. Kokubo, M.H. Kim, N. Forest, *In vitro* bone formation on a bone like apatite layer prepared by a biomimetic process on a bioactive glass–ceramic, Biomed. Mater. Res. 49 (2000) 423–434.
[22] C. Ohtsuki, T. kokubo, T. Yamammuro, Mechanism of apatite formation on CaO–SiO_2–P_2O_5 glasses in a simulated body fluid, J. Non-Cryst. Solids 143 (1992) 84–92.
[23] J.M. Oliveira, R.N. Correia, M.H. Fernandes, Effects of Si speciation on the *in vitro* bioactivity of glasses, Biomaterials 23 (2002) 371–379.
[24] N. Kanzaki, K. Onuma, G. Treboux, S. Tsutsumi, A. Ito, Effect of impurity on two-dimensional nucleation kinetics: case studies of magnesium and zinc on hydroxyapatite (0 0 0 1) face, J. Phys. Chem. B 105 (2001) 1991–1994.
[25] L.L. Hench, O. Peitl, G. La-Torre, E.D. Zanotto, Bioactive ceramics and method of preparing bioactive ceramics, US Patent 5,981,412 (9 November 1999).